Analytic expression for the charge carried by a locally excited Bloch state

István Magashegyi,[1] Katalin Oltyán,[1] and Péter Földi [1,2,*]

[1]*Department of Theoretical Physics, University of Szeged, Tisza Lajos körút 84, H-6720 Szeged, Hungary*
[2]*ELI-ALPS, ELI-HU Non-Profit Ltd., Wolfgang Sandner utca 3, H-6728 Szeged, Hungary*

We consider the time evolution of Bloch electrons after a local excitation, like an interaction with a focused laser pulse that irradiates only a part of the sample. The disturbance caused by the excitation propagates along the sample towards detectors. We focus on the measurable time integral of the usually rapidly oscillating current. In the long time limit this integral is the total charge that is displaced by the excitation. We develop an analytic way for calculating this charge. The results are verified using an analytic example with quadratic dispersion in one dimension. Additionally, numerical calculations are also performed in order to visualize the relevant physical processes in a wide band gap material that is excited by a laser pulse.

I. INTRODUCTION

Quantum mechanical particles moving in periodic potentials are of interest since the advent of quantum theory. The standard example is clearly the dynamics of electrons in a crystal lattice, but new, mainly artificial systems have also appeared more recently. These include, e.g., periodic waveguide structures [1,2], periodic dielectric systems [3], or optical superlattices [4,5]. The stationary states of these systems, the Bloch states, are delocalized with their spatial extension being the same as that of the whole sample. Although it is possible to excite the complete system in a spatially uniform way, it is more realistic to consider an interaction, e.g., with an external field that involves only a part of the sample. (This does not necessarily mean that the dipole approximation is invalid, e.g., the linear size of the focal spot for a laser beam in the visible range is at least three orders of magnitude larger than typical solid state lattice constants.) The spatially localized excitation produces disturbances (quantum mechanical wave packets) that propagate away the interaction area. In the following we focus on the dynamics of these wave packets. Our results based on Bloch states provide building blocks for the description of more general initial states.

Although the methods to be presented here have various applications, our main motivation and the context of the presentation will be the interaction of solids with pulsed laser fields. Laser pulses impinging on solid state targets can induce currents, even in dielectrics, as demonstrated in Ref. [6]. Pulsed sources can produce bursts of electromagnetic radiation with a duration in the femtosecond domain, thus the interaction is finite not only in space, but also in time. For time-dependent excitations, optical methods offer arguably the shortest available switching times [7].

On the other hand, currently available detectors cannot resolve such fast dynamics. It is only the time integral of the light-induced current (i.e., the charge displaced by the laser pulse) that can be measured. Considering a light-induced, moving electron wave packet, one can calculate the corresponding time-dependent current that flows through a given, fixed surface. By integrating this current, the charge that can be collected along the surface is obtained. This method is relatively straightforward, although the actual calculations usually can only be performed numerically. Since it is the calculation of the time evolution that is numerically expensive, it is worth obtaining the charge without the explicit need of the time-dependent wave functions, as allowed by a Fourier-transform-based method to be presented here.

Considering the light-induced process itself, various approaches can be used for calculating the dynamics. There are related time-dependent numerical methods based on the single-particle Schrödinger equation [8–10], Green's functions [11], and semiconductor Bloch equations [12–17] (possibly supplemented by terms analogous to that of the Boltzmann equation for interband dynamics [18]) are also found to be effective. However, the charge displaced by the laser pulse is typically detected considerably after the pulse and far away from the interaction area. In other words, the laser pulse creates a nonequilibrium charge distribution, the free time evolution (when the pulse is over) of which is to be calculated in order to determine the displaced charge. Obviously when the external field is zero, there are no issues that are related to the choice of the electromagnetic gauge [19,20].

The complete description of the problem would require a numerically demanding multiparticle model, including electron correlations. However, as it is shown, e.g., by Refs. [21–26], single-electron calculations can adequately reproduce the steady state quantum transport properties of various systems, and dynamical models with time-dependent bias or external fields are also successful in this regime [11,27,28]. In view of this, as a first step, in the following we also apply a single-electron model. We assume that the states that result from the local optical excitation of electrons are known and

*foldi@physx.u-szeged.hu

they are described by a superposition of Bloch states. This initial condition is used for the analytic determination of the charge displaced by the laser pulse. In this picture the sum of the contributions corresponding to all Bloch states that are populated before the arrival of the laser pulse provides the net charge displaced by the laser pulse. A similar summation was shown to lead [29] to an elegant, easily computable expression for the transferred charge in terms of higher order susceptibilities. (But, by necessity, without the insight to the electron dynamics to be provided here.) Besides the context outlined above, a simplified version of our method (with plane waves instead of Bloch states) can be applied, e.g., for a particle beam that propagates in free space with low momentum uncertainty, see, e.g., Refs. [30–33].

In the following, in Sec. II we outline the problem, the analytic solution of which is given in Sec. III. The results are compared to analytically solvable and numerical examples in Sec. IV. Conclusions are drawn in Sec. V.

II. MOTIVATION AND STATEMENT OF THE PROBLEM

For calculating the current $I(T)$ that flows through a ballistic sample (e.g., InAlAs/InGaAs based heterostructure) at a temperature T, a widely used method [21] is based on the expression

$$I(T) = \int i(\mathcal{E}) f(\mathcal{E}, T) d\mathcal{E}, \qquad (1)$$

where integration is over the possible electron energies $\mathcal{E}$, while $f(\mathcal{E}, T)$ is the Fermi function and $i(\mathcal{E})$ denotes the contribution of states with energy $\mathcal{E}$ to the net current. (Since these currents are usually measured in the output leads, we omitted the spatial arguments here.) That is, for static external interactions (caused by, e.g., gate voltages), the currents carried by the energy eigenfunctions are to be calculated. (These states—due to the possible external gates—are generally not Bloch states, and the corresponding currents are usually calculated using the Landauer-Büttiker [34,35] method.)

For time-dependent excitations, a similar expression holds:

$$I(T, t, \mathbf{r}) = \int i(\mathcal{E}, t, \mathbf{r}) f(\mathcal{E}, T) d\mathcal{E}, \qquad (2)$$

but in this case $i(\mathcal{E}, t, \mathbf{r})$ denotes the current that is carried by states that are injected in the sample at energy $\mathcal{E}$ [11]. [$I(T, t, \mathbf{r})$, as indicated by the arguments, generally depends on both space and time.] Without external influence (no gate voltages, no laser excitation), these are also energy eigenstates in the sample itself, with appropriate (transparent) boundary conditions. This emphasizes the role of Bloch states in calculating the time-dependent net current.

Considering optical excitation, the sampling time of state-of-the-art charge detectors can be by orders of magnitude longer than the characteristic time of charge oscillations. In order to calculate experimentally measurable results, we are to determine the charges displaced by the laser pulse in the long time limit. As we demonstrate, the assumption $t \to \infty$ renders the problem analytically solvable.

Let us consider an electron described by a Bloch state

$$\Psi_n(\mathbf{k}, \mathbf{r}) = \frac{1}{\sqrt{N}} u_n(\mathbf{k}, \mathbf{r}) e^{i\mathbf{k}\mathbf{r}}. \qquad (3)$$

Since in the following the reciprocal space will be considered to be continuous, we wrote $\mathbf{k}$ as an argument, while n denotes the band index. We use the convention that the lattice periodic parts of the Bloch states are normalized in a unit cell of volume V_c, i.e.,

$$\int_{V_c} u_{n'}^*(\mathbf{k}, \mathbf{r}) u_n(\mathbf{k}, \mathbf{r}) d^3\mathbf{r} = \delta_{nn'}. \qquad (4)$$

This means that the constant $N = V/V_c$ appearing in $\Psi_n(\mathbf{k}, \mathbf{r})$ provides the normalization of the Bloch states over the complete crystal volume, V. Note that with this normalization condition, the dimension of the wave function (m$^{-3/2}$) is carried by the periodic part $u_n(\mathbf{k}, \mathbf{r})$ of the Bloch states.

In view of the beginning of this section, it is worth focusing on a single Bloch state. Let $\Psi_{n_0}(\mathbf{k}_0, \mathbf{r})$ denote the state that is being excited locally, e.g., by a laser pulse. Assuming that the exciting interaction has a finite duration, after the excitation, the state of the electron can be written generally as

$$\Psi(\mathbf{r}, t) = \Psi_{n_0}(\mathbf{k}_0, \mathbf{r}, t) + \Phi(\mathbf{r}, t), \qquad (5)$$

i.e., we can separate the time evolution of the initial state. This is motivated by the intention of focusing on effects caused by the laser pulse, i.e., on the state $\Phi(\mathbf{r}, t)$ that emerges as a consequence of the light-matter interaction. Additionally, if a solid state system was in thermal equilibrium before the interaction with the laser pulse, the net current carried by the states $\Psi_{n_0}(\mathbf{k}_0, \mathbf{r}, t)$ and $\Psi_{n_0}(-\mathbf{k}_0, \mathbf{r}, t)$ would always be zero.

In the following we consider $\Phi(\mathbf{r}, t)$ as a given, known complex valued function. In other words, we concentrate on the time evolution *after* the pulse (when the external electric field is zero). In view of this, it is natural to consider the end of the laser excitation as $t = 0$. For $t > 0$, since $\Psi_{n_0}(\mathbf{k}_0, \mathbf{r}, t)$ is an eigenfunction of the field-free Hamiltonian of the system, we have

$$\Psi_{n_0}(\mathbf{k}_0, \mathbf{r}, t) = \Psi_{n_0}(\mathbf{k}_0, \mathbf{r}, 0) e^{-i\frac{\mathcal{E}_{n_0}(\mathbf{k_0})}{\hbar} t}$$
$$= \Psi_{n_0}(\mathbf{k}_0, \mathbf{r}, 0) e^{-i\omega_{n_0}(\mathbf{k_0})t}, \qquad (6)$$

where $\mathcal{E}_{n_0}(\mathbf{k}) = \hbar\omega_{n_0}(\mathbf{k})$ denotes the dispersion of the n_0th band. Now it is convenient to expand $\Phi(\mathbf{r}, t = 0)$ also in the basis of Bloch states:

$$\Phi(\mathbf{r}, t = 0) = \sum_n \int_{BZ} \phi_n(\mathbf{k}) \Psi_n(\mathbf{k}, \mathbf{r}) d^3\mathbf{k}, \qquad (7)$$

where $\phi_n(\mathbf{k})$ denotes the "expansion coefficients," and the integral runs over the first Brillouin zone. Note that the normalizability of the Bloch states (3) requires us to consider a finite sample, when the reciprocal space contains densely situated, but discrete points. Above we applied the usual approximation of replacing a sum over the discrete points by an integral.

The expansion (7) leads to

$$\Phi(\mathbf{r}, t) = \sum_n \int_{BZ} \phi_n(\mathbf{k}) e^{-i\omega_n(\mathbf{k})t} \Psi_n(\mathbf{k}, \mathbf{r}) d^3\mathbf{k}. \qquad (8)$$

The usual nonrelativistic, field-free probability current density is given by

$$\mathbf{j}(\mathbf{r}, t) = \frac{\hbar}{m} \text{Im} \{\Psi^*(\mathbf{r}, t) \nabla \Psi(\mathbf{r}, t)\}. \qquad (9)$$

By substituting the decomposition (5) into the equation above, we can separate three different terms. For example, for the x component of this current density we have

$$
j_x(\mathbf{r}, t) = \underbrace{\frac{\hbar}{m} \operatorname{Im} \left\{ \Psi_{n_0}^*(\mathbf{k}_0, \mathbf{r}, t) \frac{\partial \Psi_{n_0}(\mathbf{k}_0, \mathbf{r}, t)}{\partial x} \right\}}_{j_0(\mathbf{r}, t)} + \underbrace{\frac{\hbar}{m} \operatorname{Im} \left\{ \Phi^*(\mathbf{r}, t) \frac{\partial \Phi(\mathbf{r}, t)}{\partial x} \right\}}_{j_\Phi(\mathbf{r}, t)}
$$
$$
+ \underbrace{\frac{\hbar}{m} \operatorname{Im} \left\{ \Psi_{n_0}^*(\mathbf{k}_0, \mathbf{r}, t) \frac{\partial \Phi(\mathbf{r}, t)}{\partial x} + \Phi^*(\mathbf{r}, t) \frac{\partial \Psi_{n_0}(\mathbf{r}, t)}{\partial x} \right\}}_{j_c(\mathbf{r}, t)}. \tag{10}
$$

Here the probability current density $j_0(\mathbf{r}, t)$ corresponds to $\Psi_{n_0}(\mathbf{k}_0, \mathbf{r}, t)$, $j_\Phi(\mathbf{r}, t)$ belongs to $\Phi(\mathbf{r}, t)$, while $j_c(\mathbf{r}, t)$ is the cross term. (For the sake of brevity, we omitted the index x here.) The probability current $I(x, t)$ flowing through a surface that is parallel to the y-z plane is the integral of j_x (10) along the surface. Clearly the probability current density and the charge current density are proportional. For the sake of simplicity, we use the term "charge" for the time integral of the probability current I.

We assume that the detectors start collecting charges at $t = 0$, that is, the measured charge is zero everywhere at this time instant (and before). The charge Q_0 originating from j_0 is linearly increasing/decreasing in time at any given position of the detection plane. [However, in solid state targets, this will not lead to a detectable charge at all, since the constant, equilibrium j_0 is exactly compensated by a current related to the Bloch state $\Psi_{n_0}(-\mathbf{k}_0, \mathbf{r}, t)$.] We are to determine the additional charge that stems from the presence of $\Phi(\mathbf{r}, t)$. That is, we will calculate the difference:

$$
Q_d(x, t \to \infty) = Q_d(x)
$$
$$
= \int_0^\infty I(x, t) - I_0(x, t)\, dt
$$
$$
= \underbrace{\int_0^\infty I_\Phi(x, t)\, dt}_{Q_\Phi(x)} + \underbrace{\int_0^\infty I_c(x, t)\, dt}_{Q_c(x)}. \tag{11}
$$

For the sake of simplicity, above we assumed that the detection plane can be described as x being fixed. Generalization for differently oriented detection planes is straightforward.

III. ANALYTIC SOLUTION

A. The general case in one dimension

Although there is no fundamental difficulty in performing the calculations in three dimensions, it is more transparent to consider the problem in one dimension (1D) only. This approach allows us to see the most important conceptual steps without the need of performing multidimensional integrals. The generalization of the calculations to be presented below to the three-dimensional case can be found in the Appendix.

In 1D there is no need to perform spatial integration along the "detection surface," which reduces to a single point in this

case. Let us start with $Q_\Phi(x)$:

$$
Q_\Phi(x) = \frac{\hbar}{m} \operatorname{Im} \left\{ \sum_{n, n'} \int_0^\infty \int_{\mathrm{BZ}} \int_{\mathrm{BZ}} e^{-i[\omega_{n'}(k') - \omega_n(k)]t} \right.
$$
$$
\left. \times \phi_n^*(k)\phi_{n'}(k')\Psi_n^*(k, x) \frac{\partial \Psi_{n'}(k', x)}{\partial x}\, dk\, dk'\, dt \right\}. \tag{12}
$$

The integrals can be simplified using the identity

$$
\int_0^\infty e^{-i[\omega_{n'}(k') - \omega_n(k)]t}\, dt = \pi \delta[\omega_{n'}(k') - \omega_n(k)]
$$
$$
- \frac{i}{\omega_{n'}(k') - \omega_n(k)}, \tag{13}
$$

where a Dirac-delta distribution appears and a Cauchy principle value is understood on the right-hand side. Let us use the notation $Q_\Phi(x) = Q_\Phi'(x) + Q_\Phi''(x)$, where $Q_\Phi'(x)$ corresponds to the case when the first term of Eq. (13) is being inserted into Eq. (12), while the principal value integral appears in $Q_\Phi''(x)$.

In order to proceed, we need some pieces of information regarding the dispersion relation of the system. By assuming direct band gaps, $\delta[\omega_{n'}(k') - \omega_n(k)]$ does not give any contribution for different band indices n and n'. (This certainly holds in 1D, but as we show in the Appendix, it is also true in three-dimensional calculations.) Clearly the condition $\omega_n(k') = \omega_n(k)$ trivially holds for $k = k'$, but this is not the only possibility. For example, $\omega_n(k) = \omega_n(-k)$ for Bloch electrons. For the sake of simplicity, in the following we will consider only these two cases. This leads to

$$
Q_\Phi'(x) = \frac{\hbar}{m} \operatorname{Im} \left\{ \pi \sum_n \int_{\mathrm{BZ}} \frac{|\phi_n(k)|^2}{|\omega_n'(k)|} \Psi_n^*(k, x) \frac{\partial \Psi_n(k, x)}{\partial x}\, dk \right.
$$
$$
\left. + \pi \sum_n \int_{\mathrm{BZ}} \frac{\phi_n^*(k)\phi_n(-k)}{|\omega_n'(-k)|} \Psi_n^*(k, x) \frac{\partial \Psi_n(-k, x)}{\partial x}\, dk \right\}, \tag{14}
$$

where $\omega_n'(k) = \frac{\omega_n(k')}{\partial k'}\big|_{k'=k}$, i.e., the velocity in the nth band at k. Since $\Psi_n(-k, x) = \Psi_n^*(k, x)$, the imaginary part of the second term above is zero, thus it does not give contribution to Q_Φ. Additionally, it is worth averaging Q_Φ over a unit cell of length a that contains x, by calculating

$$
\overline{Q_\Phi'}(x) = \frac{1}{a} \int_{x-a/2}^{x+a/2} Q_\Phi'(s)\, ds. \tag{15}
$$

This averaging allows us to introduce the band velocity $\omega_n'(k)$. The known expectation value of the momentum in a Bloch state is

$$\int_{-L/2}^{L/2} \Psi_n^*(k,x)(-i\hbar)\frac{\partial \Psi_n(k,x)}{\partial x}dx = m\omega_n'(k). \quad (16)$$

As it can be shown easily, by integrating over a unit cell only (instead of the whole 1D crystal of length L), we obtain a result that is less by a factor of N, that is, by the number of unit cells in the crystal [see Eqs. (3) and (4) for the normalization]:

$$\frac{\hbar}{m}\int_{-a/2}^{a/2} \Psi_n^*(k,x)\frac{\partial \Psi_n(k,x)}{\partial x}dx = \frac{i}{N}\omega_n'(k). \quad (17)$$

Substituting this result into the expression for $\overline{Q_\Phi'}$, finally we obtain

$$\overline{Q_\Phi'} = \frac{\pi}{L}\sum_n \int_{\mathrm{BZ}} \mathrm{sgn}[\omega_n'(k)]|\phi_n(k)|^2\,dk, \quad (18)$$

where $L = Na$ were used. $\overline{Q_\Phi'}$ is independent of x, which is a consequence of Eq. (17).

The integral in Q_Φ'' with respect to k' can also be simplified, provided we can use reasonable assumptions on the analytic properties of the integrand as a complex function. Clearly when, e.g., a numerical calculation provides the coefficients $\phi_n(k)$, there is no strict way of extending the integrand to the whole complex plane. However, in dipole approximation "all transitions are vertical." When the excitation is local, but the interaction volume is much larger than a unit cell, a similar result is expected, i.e., a narrow final distribution around k_0. Practically we may assume that the modulus of the "expansion coefficients" $|\phi_n(k)|$ has a finite support in k for all bands. This allows us to extend the integration limits to $\pm\infty$ along the real axis and consider closing the contour. To this end we are to investigate the term $\exp(ik'x)$ which is the plane wave part of $\Psi_n(k',x)$. For positive values of x, if k' has positive imaginary part, this term exponentially decreases as $\mathrm{Im}(k') \to \infty$. If this is the dominant term in the integrand, we can close the contour on the upper half plane. (Let us denote this contour by Ω_+.) While being reasonable, at this point this is certainly an assumption. (Numerical results, however, support this assumption, see the next section.) By closing he contour we obtain

$$Q_\Phi''(x) = \mathrm{Im}\left\{ \frac{-i\hbar}{m}\sum_{n,n'}\int_{\mathrm{BZ}}\oint_{\Omega_+}\frac{\phi_n^*(k)\phi_{n'}(k')}{\omega_{n'}(k')-\omega_n(k)} \right.$$
$$\left. \times \Psi_n^*(k,x)\frac{\partial \Psi_{n'}(k',x)}{\partial x}\,dk'\,dk \right\}$$
$$= \mathrm{Im}\left\{ \sum_{n,n'}\int_{\mathrm{BZ}}\oint_{\Omega_+}\frac{\mathcal{N}(k,k',x)}{\omega_{n'}(k')-\omega_n(k)}\,dk'\,dk \right\}. \quad (19)$$

For $n = n'$, the integrand has two poles ($k' = \pm k$) along the integration path (on the real axis). Assuming that these poles are simple, they can be accounted for by calculating $i\pi$ times the corresponding residue $\mathcal{N}(k,k,x)/\omega_n'(k)$ and $\mathcal{N}(k,-k,x)/\omega_n'(-k)$. When $n \neq n'$, and we consider the case of direct band gaps, there is no real solution k' of the equation $\omega_{n'}(k') = \omega_n(k)$. There can be poles, however, in the upper

half plane, but their contributions vanish for large positive values of x, which correspond to the physically reasonable scenario of distant detectors. In this case we have

$$Q_\Phi''(x_0) = \frac{\hbar}{m}\,\mathrm{Im}\left\{ \pi\sum_n\int_{\mathrm{BZ}}\frac{|\phi_n(k)|^2}{\omega_n'(k)}\Psi_n^*(k,x)\frac{\partial \Psi_n(k,x)}{\partial x}\,dk \right.$$
$$\left. +\pi\sum_n\int_{\mathrm{BZ}}\frac{\phi_n^*(k)\phi_n(-k)}{\omega_n'(-k)}\Psi_n^*(k,x)\frac{\partial \Psi_n(-k,x)}{\partial x}\,dk \right\}, \quad (20)$$

which is the same as Eq. (14) except from the denominator. The imaginary part of the second term is zero also in this case. Following the same steps that led us to Eq. (18) from Eq. (14), we can calculate a cell-averaged charge $\overline{Q_\Phi''}$. Combining with Eq. (18), we have, for large positive values of x:

$$\overline{Q_\Phi}(x \to \infty) = \frac{\pi}{L}\left(\sum_n\int_{\mathrm{BZ}}(1+\mathrm{sgn}[\omega'(k)])\,|\phi_n(k)|^2\,dk \right)$$
$$= \frac{2\pi}{L}\sum_n\int^+ |\phi_n(k)|^2\,dk, \quad (21)$$

where the symbol $\int^+$ refers to integration over the domain where $\omega_n'(k)$ is positive. Similarly, for negative, but large magnitude values of x (when we can close the contour on the lower half plane leading to a clockwise oriented integration path) we obtain

$$\overline{Q_\Phi}(x \to -\infty) = -\frac{2\pi}{L}\sum_n\int^- |\phi_n(k)|^2\,dk. \quad (22)$$

These are very intuitive results, telling us that the charge carried by a laser-induced wave packet $\Phi(x)$ in the positive (negative) direction is proportional to its part that corresponds to positive (negative) band velocities. Additionally, the contributions of different bands are found to be decoupled.

Considering the term Q_c, which stems from the cross term of the the initial state and the wave packet $\Phi(x)$, we can follow similar steps as above, and obtain

$$\overline{Q_c}(x \to \infty) = \frac{4\pi}{L}\,\mathrm{Re}\{\phi_{n_0}(k_0)\}, \quad (23)$$

provided $\omega_{n_0}'(k_0) > 0$ and zero otherwise. [Let us recall that the initial state is $\Psi_{n_0}(k_0,x)$.] Similarly, for $x \to -\infty$ we have the nonzero contribution of

$$\overline{Q_c}(x \to -\infty) = -\frac{4\pi}{L}\,\mathrm{Re}\{\phi_{n_0}(k_0)\} \quad (24)$$

only for negative initial band velocity $\omega_{n_0}'(k_0)$. Combining the last formulas of $Q_\Phi(x)$ and $Q_c(x)$ above leads to the final result. For $x \to \infty$ we have

$$\overline{Q_d}(x \to \infty) = \frac{2\pi}{L}\sum_n\int^+ |\phi_n(k)|^2\,dk$$
$$+ \begin{cases} \frac{4\pi}{L}\,\mathrm{Re}\{\phi_{n_0}(k_0)\} & \text{if } \omega_{n_0}'(k_0) > 0, \\ 0 & \text{otherwise,} \end{cases} \quad (25)$$

and for the opposite, negative direction we have

$$\overline{Q_d}(x \to -\infty) = -\frac{2\pi}{L} \sum_n \int^- |\phi_n(k)|^2 \, dk$$
$$- \begin{cases} \frac{4\pi}{L} \operatorname{Re}\{\phi_{n_0}(k_0)\} & \text{if } \omega'_{n_0}(k_0) < 0, \\ 0 & \text{otherwise.} \end{cases} \quad (26)$$

These equations mean that in the $x \to \infty$ ($x \to -\infty$) limit: (i) only the part of the laser-induced "disturbance" $\Phi(x)$ plays a role that corresponds to positive (negative) band velocities, and (ii) the initial state $\Psi_{n_0}(k_0, x)$ contributes to the measurable charge also only if its band velocity is positive (negative). This provides a very transparent physical picture.

Let us note that in the calculations above the expansion coefficients $\phi_n(k)$ played a crucial rule. It is not only the magnitudes of these complex valued functions that influence the final result, their phases are equally important. When calculating the laser-induced dynamics (which is not the topic of the current paper), these phases strongly depend on the phases of the matrix elements of the light-matter interaction term in the Hamiltonian. This underlines the importance of the phases of the "transition dipole matrix elements" during the light-induced time evolution [36].

B. The case of quadratic dispersion

An important example when not only the limits $x \to \pm\infty$ can be obtained analytically, is the case of quadratic dispersion. For the sake of simplicity we present the calculations for a single band. As we shall see, by using effective mass approximation [when $\omega(k) = \frac{\hbar}{2m^*}k^2 + \omega_0$] there is no need for assuming analytic properties of the integrands, simple algebraic calculations suffice. Since we focus on a single band, we can drop the band indices and write the initial state as

$$\Psi(x, 0) = \Psi_0(x) + \Phi(x) = \frac{1}{\sqrt{L}}\left[e^{ik_0 x} + \int_{-\infty}^{\infty} e^{ikx} \phi(k) dk \right]. \quad (27)$$

Note that here we assumed that the distribution $\phi(k)$ is narrow enough so that the dispersion is quadratic all over the support of $\phi(k)$. This allows us to safely extend the limits of the integral to $\pm\infty$. For the sake of comparison, we kept the normalization convention given by Eqs. (3) and (4). This means that the inverse of the Fourier transform above is given by

$$\phi(k) = \frac{\sqrt{L}}{2\pi} \int_{-\infty}^{\infty} e^{-ikx} \Phi(x) dx. \quad (28)$$

With these conventions, the real and reciprocal space probability densities read $\rho(x) = |\Psi(x, 0)|^2$, $\tilde{\rho}(k) = 2\pi/L|\phi(k)|^2$. (The dimensions of these 1D quantities are the usual, i.e., $1/m$ and m, respectively.)

In this case there is no need to perform averaging over a unit cell, we can calculate the position dependent charges directly. Most terms can be evaluated in a straightforward way,

it is only

$$Q''_\Phi(x) = \frac{2m^*}{Lm} \operatorname{Im}\left\{ \int_{-\infty}^{\infty} \int_{-\infty}^{\infty} ik' \frac{\phi^*(k)\phi(k')}{(k'^2 - k^2)} e^{i(k'-k)x} \, dk \, dk' \right\} \quad (29)$$

that requires special attention. Now we can use the partial fraction decomposition $k'/(k'^2 - k^2) = \frac{1}{2}[1/(k - k') - 1/(k + k')]$. As it can be seen, the imaginary part of the integral with a denominator of $k + k'$ vanishes. That is,

$$Q''_\Phi(x) = -\frac{m^*}{Lm} \operatorname{Im}\left\{ \int_{-\infty}^{\infty} \int_{-\infty}^{\infty} i\frac{\phi^*(k)\phi(k')}{k' - k} e^{i(k'-k)x} \, dk \, dk' \right\}. \quad (30)$$

This result can be simplified further by using the following identity (which can be obtained by using the Fourier transform of the Heaviside step function):

$$\frac{e^{i(k'-k)x}}{k' - k} = -i\pi \delta(k' - k) + i \int_{-\infty}^{x} e^{i(k'-k)s} \, ds. \quad (31)$$

This leads to the following integrals:

$$Q''_\Phi(x) = -\frac{\pi m^*}{Lm} \int_{-\infty}^{\infty} |\phi(k')|^2 \, dk'$$
$$+ \frac{m^*}{Lm} \int_{-\infty}^{x} \left| \int_{-\infty}^{\infty} \phi(k) e^{iks} \, dk \right|^2 ds. \quad (32)$$

Combining this with the expression for $Q'_\Phi(x)$ leads to

$$Q_\Phi(x) = -\frac{m^*}{m} \int_{-\infty}^{0} \tilde{\rho}(k) \, dk + \frac{m^*}{m} \int_{-\infty}^{x} \rho(s) \, ds. \quad (33)$$

Note that in spite of the apparent distinguished role of negative values of k above, the sign of k has no physical significance, it is simply a consequence of a choice in (31). Using a similar identity with different signs and integration limits, we would have obtained

$$Q_\Phi(x) = \frac{m^*}{m} \int_{0}^{\infty} \tilde{\rho}(k) \, dk - \frac{m^*}{m} \int_{x}^{\infty} \rho(s) \, ds, \quad (34)$$

which is equivalent to Eq. (33). For the sake of definiteness, Eq. (33) will be used in the following.

Following similar steps, the charge related to the cross term can also be calculated. Finally, we obtain

$$Q_d(x) = -\frac{m^*}{m} \int^- \tilde{\rho}(k) \, dk + \frac{m^*}{m} \int_{-\infty}^{x} \rho(s) \, ds$$
$$+ 2\operatorname{Re}\left\{ \frac{1}{\sqrt{L}} \int_{-\infty}^{x} \Phi(x') e^{-k_0 x'} \, dx' \right\}$$
$$- \begin{cases} \frac{4\pi}{L} \operatorname{Re}\{\phi(k_0)\} & \text{if } k_0 < 0, \\ 0 & \text{otherwise.} \end{cases} \quad (35)$$

As direct calculations in the $x \to \pm\infty$ limits show, this result is consistent with the ones given by Eqs. (25) and (26).

IV. ANALYTIC AND NUMERICAL EXAMPLES

The expressions (25), (26), and (35) mean the central results of this paper. In this section we present examples that verify these analytic findings and also point out their possible

applications. First we consider the case of a Gaussian wave packet, for which the time integral of the corresponding current can be calculated in a way that is completely independent from equations we obtained so far. This allows a direct, analytic verification of our results for a single band. For two bands we calculate numerically the current that is induced by a laser pulse that excites an initial Bloch state. In 1D it is also possible to obtain Q_d by direct time domain integration, which, for distances far away the interaction area, is directly comparable to the results given by Eqs. (25) and (26). The agreement that we found is convincing.

A. Gaussian wave packet

Wave packets, the time evolution of which are well known, allow the calculation of the charge Q_d analytically, i.e., independently from the previous calculations. This offers a possibility to validate our result (35) that is related to the case of quadratic dispersion and plane wave expansion (27) for a single band. Along this line, let us consider the case when the additional wave packet $\Phi(x)$ is a normalized Gaussian with uncertainty σ_x and expectation value x_G:

$$\Phi(x) = \frac{1}{\sqrt{\sqrt{2\pi}\sigma_x}} \exp\left(-\frac{(x-x_G)^2}{4\sigma_x^2} + i k_G (x-x_G)\right).$$

(36)

Let us emphasize that there is little chance that, e.g., laser excitation creates a wave packet which is exactly a Gaussian, it is the analyticity of the time evolution that makes this example worth investigating.

The charge carried by the Gaussian (36) in the $t \to \infty$ limit can be computed in two different ways. We can use the wave function in momentum representation and apply Eq. (35), but the known time evaluation of a Gaussian wave packet together with the continuity equation also provides an analytic result. Both approaches lead to

$$Q_\Phi(x) = \frac{1}{2}\text{erf}\left(\frac{x-x_G}{\sqrt{2}\sigma_x}\right) + \frac{1}{2}\text{erf}\left(\frac{k_G}{\sqrt{2}\sigma_k}\right).$$

(37)

We also obtain the same expression for the cross-term Q_c using both methods:

$$Q_c(x) = \frac{\sqrt{2\pi}}{\sqrt{\sqrt{2\pi}\sigma_k}} \exp\left(-\frac{(k_0-k_G)^2}{4\sigma_k^2}\right)$$

$$\times \left[\text{sgn}(k_0) \cos(k_0 x_G) \right.$$

$$\left. + \text{Re}\left\{ e^{-ik_0 x_G}\text{erf}\left(\frac{x-x_G}{2\sigma_x} + i\frac{k_0-k_G}{2\sigma_k}\right)\right\}\right], \quad (38)$$

where k_0 corresponds to the initial plane wave. Clearly the final result $Q_d(x)$ is the sum of Eqs. (37) and (38).

We illustrate the formulas by considering four different cases, when both x_G and k_G are either close to zero or have considerably larger values, see Fig. 1. As a common feature of the results shown by Fig. 2, we can observe that there is a relatively sudden (as wide as σ_x) change in Q_d around $x = x_G$. This effect is related to Q_Φ, since this is the range where the first term in Eq. (37) changes the most significantly.
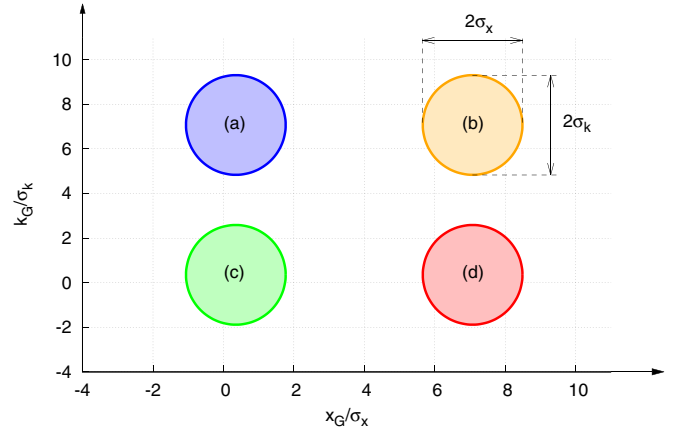

FIG. 1. In order to illustrate the effect of different parameters on Q_d, we consider Gaussian wave packets that are superimposed on an initial plane wave. The figure shows the parameters of the four different Gaussians to be investigated.

This term is dominant when k_G is close to zero, therefore Q_d changes sign in cases (c) and (d). We can also see that the magnitude of Q_d is the largest along the line described by $k_0 = k_G$. This is a consequence of the Gaussian factor in Q_c. The oscillatory patterns that are more pronounced for cases (b) and (d) also originate from the cross term Q_c, they are induced by the factors $\cos(k_0 x_G)$. This explains why these oscillations are less visible in cases (a) and (c) when the "wavelength" of the oscillations is longer and only a few periods appear before they decay.
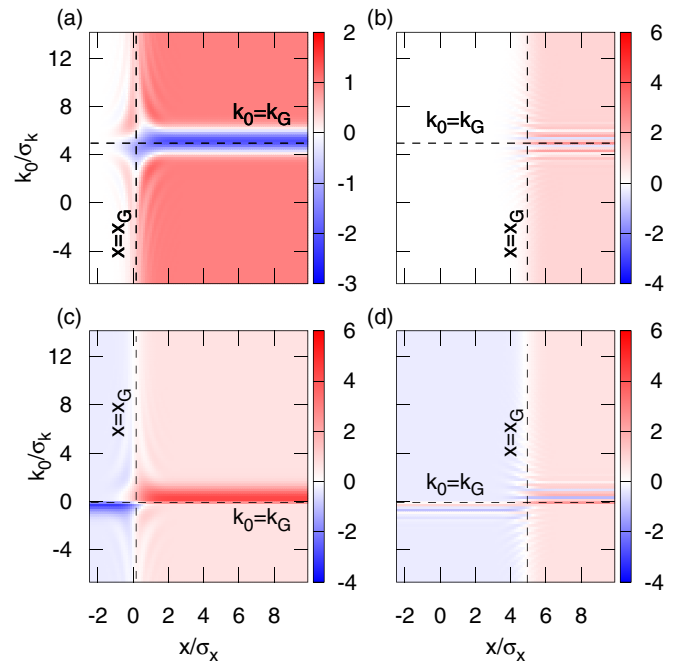

FIG. 2. Q_d for Gaussian wave packets with different parameters. (a)–(d) Cases that are denoted by the same letters in Fig. 1. The plots were drawn using Eq. (35), but direct analytical calculations lead to exactly the same result.

B. Numerical example: External pulse induced localized excitations

In the previous subsection an example was presented when—for a single band—Eq. (35) was reproduced using a conventional method. Now we carry out numerical calculations that can illustrate a practical application of our approach: optical excitation of a solid state sample.

The fact that strong, short laser pulses can lead to temporal "metallization" [37] and displace charges in a dielectric, was demonstrated in Ref. [6]. In this experiment, the edge of a silica prism was illuminated using a short (sub-4-fs) pulse at $\lambda \approx 750$ nm with peak field strength of 1.7×10^{10} V/m. The generated charges were collected by gold contacts and their time integral was measured by a current-voltage converter. When the polarization of the electric field of the pulse was perpendicular to the slit between the gold contacts, the generated charge carriers entered the contacts and produced measurable charges that depended on the carrier-envelope phase (CEP) of the pulse. More recently, considerably weaker pulses were also shown to produce similar effects. As reported in [38], for pulse energies in the pJ regime, an optimized lock-in amplification technique can also lead to CEP-dependent signals.

For the sake of simplicity, we use a two-band, 1D model for the solid. Realistically we assume that the external electromagnetic pulse is localized and has a finite duration. Previously we assumed that the initial time instant for the field-free time evolution is $t = 0$, therefore the pulse starts at $t = -\tau$ and after $t = 0$ the external field is zero. In the interaction region, the Hamiltonian describing the dynamics is given by

$$H(x,t) = \frac{1}{2m}[p - eA(x,t)]^2 + U(x,t), \qquad (39)$$

where e and m denote the charge and mass of the electron, $p = -i\hbar \frac{\partial}{\partial x}$ is the canonical momentum. U means the periodic effective potential of the crystal lattice, while $A(x,t)$ is the vector potential corresponding to the electric field $E(x,t)$ of the laser. [We assume an electric field that is linearly polarized along the x axis, and its only nonzero component is denoted by $E(x,t)$.] Outside the interaction area, $A(x,t)$ is assumed to be zero [implying $E(x,t) = -\frac{\partial}{\partial t}A(x,t) = 0$], i.e., $H = H_0 = \frac{p^2}{2m} + U(x)$ in this region. The parameters [39] of the periodic effective potential $U(x)$ are chosen so as to produce a band gap of 3.2 eV (that corresponds to the case of ZnO, which is often a target material in experiments aiming the generation of high-order harmonics [40]). The explicit form of the potential is the following:

$$U(x) = -U_0 \sum_{i=1}^{2} \cos^2[\pi(x - x_i)/\Delta], \qquad (40)$$

where $U_0^{(a)} = 25$ eV, $\Delta^{(a)}/a = 0.15$, $x_1^{(a)}/a = 0.3$, and $x_2^{(a)}/a = 0.607$ [39]. Working on a finite spatial grid, the Bloch states $\Psi_n(k,x) = 1/\sqrt{N} \exp(ikx)u_n(k,x)$ can be obtained using the eigenvalue equation

$$-\frac{\hbar^2}{2m}\left(\frac{d}{dx} + ik\right)^2 u_n(k,x) + U(x)u_n(k,x) = \mathcal{E}_n(k)u_n(k,x). \qquad (41)$$
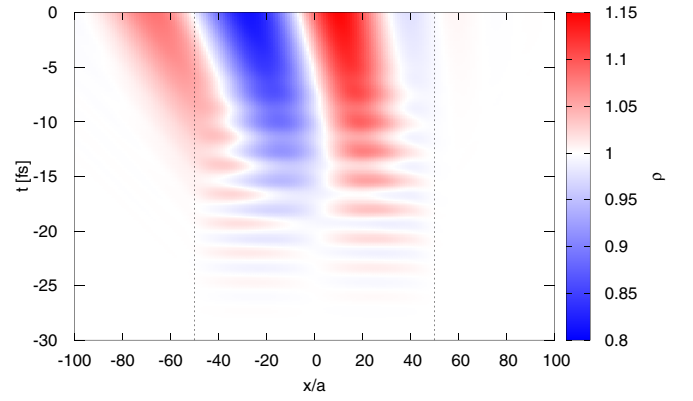

FIG. 3. Numerically calculated time evolution of the cell-averaged particle density as induced by a localized laser pulse acting in the $x \in [-l/2, l/2]$ interval, with $l = 100a$. The periodic potential for the 1D model is given by Eq. (40). The dotted vertical lines indicate the boundaries of the interaction area. The initial Bloch state corresponds to $k_0a = 0.1$, the peak electric field is 1 GV/m and $\tau = 20\pi/\omega_0$ [see Eq. (42)]. Note that using the present normalization, $\overline{\rho}(x)$ is constant unity before the excitation. The figure clearly shows the formation of a structured wave packet the propagation of which leads to Q_d that will be shown in Fig. 4.

Although it is known that in order to obtain a qualitatively correct model, many bands are needed [10], for our current demonstrative purposes it is sufficient to use the two bands (denoted by $n = 0, 1$) that are closest to the band gap of 3.2 eV. The next step is to choose an initial Bloch state $\Psi_0(k_0, x)$ in the valence band and to solve the time-dependent Schrödinger equation in the presence of the laser pulse. To this end we need the waveform of the electric field, which can be obtained using

$$A(x,t) = A_0 \cos^2\left(\frac{\pi}{l}x\right)\sin^2\left(\frac{\pi}{\tau}t\right)\cos(\omega_0 t), \qquad (42)$$

provided x is in the interaction domain between $-l/2$ and $l/2$, and $t \in [-\tau, 0]$, otherwise $A(x,t) = 0$. The central wavelength of the laser is considered to be $\lambda = 800$ nm, and the actual values of parameters l and τ will be indicated in the figures and figure captions.

The dynamics is solved using a spatial grid that is considerably larger than the interaction area, ensuring that the laser-induced wave packet does not reach the boundaries of the grid during the interaction with the laser pulse. As Fig. 3 shows, the cell-averaged probability density $\overline{\rho}(x)$ is constant before the arrival of the laser pulse, as it should be. As we can see, the laser-induced excitation creates propagating disturbances. This figure corresponds to case when the classical "traverse time" (the interaction length divided by the band velocity) is considerably longer than the optical cycle time, thus it is a good approximation to describe the laser field via its ponderomotive potential [41]. This potential depletes the interaction region, and later the created density oscillations propagate away. (Note that the initial band velocity is negative in the case shown by Fig. 3.)

When the pulse is over, at $t = 0$, the complete state of the system $\Psi(x, t = 0)$ can be factorized as a sum of $\Psi_{n_0}(x, t = 0)$ and an additional part that describes the effect of the
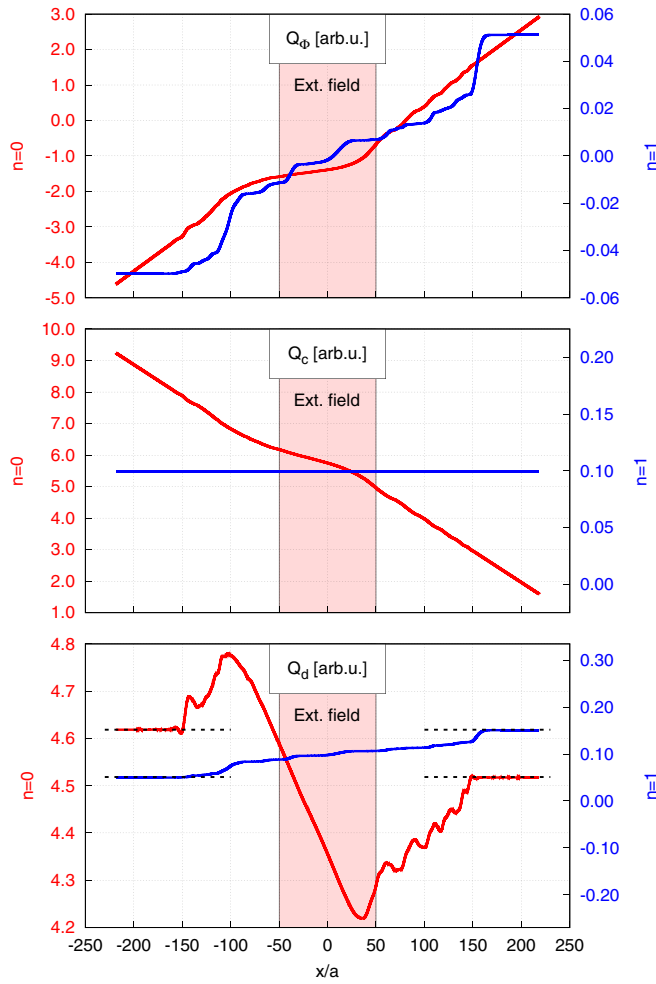
FIG. 4. Numerically obtained different components of the charge $Q_d(x)$ as a function of position. These charges result from the same excitation that induced the density oscillations shown in Fig. 3. Top panel: Q_Φ, middle panel: Q_c, bottom: their sum Q_d. The contribution of the different bands are plotted using different colors. Note that Q_c is zero for $n = 1$, since the initial state corresponded to the band $n = 0$. For Q_d, the dashed lines that are very close to the numerically obtained limiting values, show the results of Eqs. (25) and (26). The shaded domain indicated the interaction area $[-l/2, l/2]$. All parameters are the same as for Fig. 3.

excitation $\Phi(x, t = 0)$ [recall Eq. (5)]. By expanding this state in terms of the Bloch states, we can directly use Eqs. (25) and (26) to compute Q_d for large values of x.

On the other hand, we can determine the position dependence of Q_d by a direct numerical integration of the obtained current. Clearly the limit $t \to \infty$ cannot be reached numerically, but it is possible to wait until Q_d converges. The function $Q_d(x)$ that is obtained in this way (without referring to the results of Sec. III) can be seen in Fig. 4. (Note that in this figure, and also in Fig. 3, we have chosen a narrow interaction domain, which serves demonstrational purposes well, but can be difficult to realize experimentally.) As shown by Fig. 4, Q_d is constant (independent of x) far from the interaction region. In this limit, the purely numerical results and the ones obtained using Eqs. (25) and (26) coincide within a relative error of 10^{-4}. This is remarkable since the

analytic results were obtained by considering a continuous k space, while numerical integrations can only mean discrete sums. Additionally, in order to derive Eqs. (25) and (26), we applied assumptions regarding the analytic properties of the integrands. During the numerical calculations, it is impossible to imply these assumptions. This suggests that Eqs. (25) and (26) not only provide a clear physical picture for the determination of the charge displaced by a laser pulse, but they are also very general expressions.

V. CONCLUSIONS

We investigated the local excitation of charged particles in a periodic potential. The initial state of the problem is a single Bloch state, the excitation of which creates propagating wave packets. We gave a general analytic formula for the charge that is related to this disturbance. We compared our results to the analytically solvable case of a Gaussian wave packet, and found complete agreement. Numerical calculations provided similarly satisfactory verification of our approach. The results presented here can be used, e.g., in the context of optically excited solids, for understanding how the measurable electric charge that is displaced by a laser pulse depends on the parameters of the pulse.

APPENDIX: GENERALIZATION TO THREE DIMENSIONS

In three dimensions, the current that flows through a surface can be obtained by integrating the appropriate component of the current density along the surface. For the sake of simplicity, let us consider a cubic lattice, a cuboid ($L_x \times L_y \times L_z$) sample and a surface that belongs to a constant value of x. Using the notation of Sec. II, we can write

$$I(x, t) = \int_{-\frac{L_y}{2}}^{\frac{L_y}{2}} \int_{-\frac{L_z}{2}}^{\frac{L_z}{2}} j_x(x, y, z, t) dy dz = \int_{\mathcal{F}} \mathbf{j}(\mathbf{r}, t) \mathbf{n} df, \quad \text{(A1)}$$

where $\mathcal{F}$ denotes a rectangle with sides L_y and L_z and a normal vector of $\mathbf{n} = \hat{\mathbf{x}}$. Clearly

$$j_x(\mathbf{r}, t) = \frac{\hbar}{m} \text{Im} \left\{ \Psi^*(\mathbf{r}, t) \frac{\partial}{\partial x} \Psi(\mathbf{r}, t) \right\}, \quad \text{(A2)}$$

and the state $\Psi(\mathbf{r}, t)$ is given by the sum (5). It is clear that j_x contains six integrals in the k space, e.g., in Eq. (11), k and k'

have to be replaced by $\mathbf{k}$ and $\mathbf{k}'$:

$$
\begin{aligned}
Q_\Phi(x) = \frac{\hbar}{m} \, \mathrm{Im} \sum_{n,n'} \int_0^\infty \int_{\mathcal{F}} \int_{\mathrm{BZ}} \int_{\mathrm{BZ}} e^{-i[\omega_{n'}(\mathbf{k}') - \omega_n(\mathbf{k})]t} \\
\times \phi_n^*(\mathbf{k}) \phi_{n'}(\mathbf{k}') \Psi_n^*(\mathbf{k},\mathbf{r}) \frac{\partial \Psi_{n'}(\mathbf{k}',\mathbf{r})}{\partial x} \, d^3\mathbf{k} \, d^3\mathbf{k}' \, df \, dt \\
= \sum_{n,n'} \int_0^\infty \int_{\mathcal{F}} \int_{\mathrm{BZ}} \int_{\mathrm{BZ}} \mathcal{I}_{nn'}(\mathbf{k},\mathbf{k}',\mathbf{r},t) \, d^3\mathbf{k} \, d^3\mathbf{k}' \, df \, dt,
\end{aligned}
$$

where the last line only introduces a notation that simplifies the following equations. Now let us assume that the order of integration can be changed, and use that $\int_{\mathcal{F}} \mathcal{I}_{nn'}(\mathbf{k},\mathbf{k}',\mathbf{r},t) \, df$

is zero unless $k_y = k_y'$ and $k_z = k_z'$. With the appropriate prefactors, this leads to

$$
\begin{aligned}
Q_\Phi(x) = \frac{(2\pi)^2}{L_y L_z} \sum_{n,n'} \int_0^\infty \int_{\mathcal{F}} \int_{-\frac{\pi}{a}}^{\frac{\pi}{a}} \\
\times \int_{\mathrm{BZ}} \mathcal{I}_{nn'}(\mathbf{k}, k_x', \mathbf{r}, t) \, d^3\mathbf{k} \, dk_x' \, df \, dt, \quad \text{(A3)}
\end{aligned}
$$

where the integrand is a shorthand notation for $\mathcal{I}_{nn'}(k_x, k_y, k_z, k_x', k_y, k_z, \mathbf{r}, t)$ and all k-space integrals run from $-\pi/a$ to π/a. (Recall that we are considering a cubic lattice.) By changing again the order of integrals, we can write

$$
Q_\Phi(x) = \frac{(2\pi)^2}{L_y L_z} \int_{\mathcal{F}} \int_{-\frac{\pi}{a}}^{\frac{\pi}{a}} \int_{-\frac{\pi}{a}}^{\frac{\pi}{a}} \left[\sum_{n,n'} \int_0^\infty \int_{-\frac{\pi}{a}}^{\frac{\pi}{a}} \int_{-\frac{\pi}{a}}^{\frac{\pi}{a}} \mathcal{I}_{nn'}(k_x, k_y, k_z, k_x', \mathbf{r}, t) \, dk_x \, dk_x' \, dt \right] dk_y \, dk_z \, df. \quad \text{(A4)}
$$

Taking a look at the expression in the (redundant) square brackets, we can see that it is analogous to Eq. (12): Although now the functions have y, z and k_y, k_z arguments as well, while performing the integrals inside the square brackets, they can be considered as parameters. In other words, for any relevant value of y, z, k_y, k_z, we can compute the expression in the square brackets (let it be denoted by Q_Φ^{1D}) using the method introduced at the beginning of this section. That is,

$$
Q_\Phi(x) = \frac{(2\pi)^2}{L_y L_z} \int_{\mathcal{F}} \int_{-\frac{\pi}{a}}^{\frac{\pi}{a}} \int_{-\frac{\pi}{a}}^{\frac{\pi}{a}} \left[Q_\Phi^{1D}(x; y, z, k_y, k_z) \right] dk_y \, dk_z \, df.
$$
$$\text{(A5)}$$

As an illustration, let us consider the 3D analogy of Eq. (33), when the appropriate densities are $\rho(\mathbf{r}) =$

$|\Psi(\mathbf{r}, 0)|^2$, $\tilde{\rho}(\mathbf{k}) = (2\pi)^3/(L_x L_y L_z)|\phi(\mathbf{k})|^2$. Performing the calculations, we obtain

$$
Q_\Phi(x_0) = -\frac{m^*}{m} \int_{-\infty}^0 \tilde{\rho}(\mathbf{k}) \, dk_x + \frac{m^*}{m} \int_{-\infty}^{x_0} \rho(\mathbf{r}') \, dx'. \quad \text{(A6)}
$$

That is, the charge that flows through a plane that is perpendicular to the x axis and situated at a given coordinate x_0, is determined by the part of the wave packet that is characterized by $x < x_0$ and by the momentum space components for which the velocity in the x direction is negative. This is a straightforward generalization of Eq. (33): although it could have been guessed, now it is verified exactly. Equations analogous to (A5) allow us to generalize all previous results to 3D.

[1] T. Pertsch, P. Dannberg, W. Elflein, A. Bräuer, and F. Lederer, Optical Bloch Oscillations in Temperature Tuned Waveguide Arrays, Phys. Rev. Lett. **83**, 4752 (1999).

[2] R. Morandotti, U. Peschel, J. S. Aitchison, H. S. Eisenberg, and Y. Silberberg, Experimental Observation of Linear and Nonlinear Optical Bloch Oscillations, Phys. Rev. Lett. **83**, 4756 (1999).

[3] R. Sapienza, P. Costantino, D. Wiersma, M. Ghulinyan, C. J. Oton, and L. Pavesi, Optical Analogue of Electronic Bloch Oscillations, Phys. Rev. Lett. **91**, 263902 (2003).

[4] M. Ben Dahan, E. Peik, J. Reichel, Y. Castin, and C. Salomon, Bloch Oscillations of Atoms in an Optical Potential, Phys. Rev. Lett. **76**, 4508 (1996).

[5] M. Holthaus, Bloch oscillations and Zener breakdown in an optical lattice, J. Opt. B: Quantum Semiclassical Opt. **2**, 589 (2000).

[6] A. Schiffrin, T. Paasch-Colberg, N. Karpowicz, V. Apalkov, D. Gerster, S. Mühlbrandt, M. Korbman, J. Reichert, M. Schultze, S. Holzner, J. V. Barth, R. Kienberger, R. Ernstorfer, V. S. Yakovlev, M. I. Stockman, and F. Krausz, Optical-field-induced current in dielectrics, Nature (London) **493**, 70 (2013).

[7] F. Krausz and M. I. Stockman, Attosecond metrology: From electron capture to future signal processing, Nat. Photonics **8**, 205 (2014).

[8] M. Korbman, S. Y. Kruchinin, and V. S. Yakovlev, Quantum beats in the polarization response of a dielectric to intense few-cycle laser pulses, New J. Phys. **15**, 013006 (2013).

[9] M. Wu, S. Ghimire, D. A. Reis, K. J. Schafer, and M. B. Gaarde, High-harmonic generation from Bloch electrons in solids, Phys. Rev. A **91**, 043839 (2015).

[10] P. G. Hawkins, M. Y. Ivanov, and V. S. Yakovlev, Effect of multiple conduction bands on high-harmonic emission from dielectrics, Phys. Rev. A **91**, 013405 (2015).

[11] B. Gaury, J. Weston, M. Santin, M. Houzet, C. Groth, and X. Waintal, Numerical simulations of time-resolved quantum electronics, Phys. Rep. **534**, 1 (2014).

[12] H. Haug and S. W. Koch, *Quantum Theory of the Optical and Electronic Properties of Semiconductors*, 4th ed. (World Scientific, New Jersey, 2004).

[13] D. Golde, T. Meier, and S. W. Koch, High harmonics generated in semiconductor nanostructures by the coupled dynamics of

optical inter- and intraband excitations, Phys. Rev. B **77**, 075330 (2008).

[14] D. Golde, M. Kira, T. Meier, and S. W. Koch, Microscopic theory of the extremely nonlinear terahertz response of semiconductors, Phys. Status Solidi (b) **248**, 863 (2011).

[15] G. Vampa, C. R. McDonald, G. Orlando, D. D. Klug, P. B. Corkum, and T. Brabec, Theoretical Analysis of High-Harmonic Generation in Solids, Phys. Rev. Lett. **113**, 073901 (2014).

[16] G. Vampa, C. R. McDonald, G. Orlando, P. B. Corkum, and T. Brabec, Semiclassical analysis of high harmonic generation in bulk crystals, Phys. Rev. B **91**, 064302 (2015).

[17] R. Buschlinger, M. Lorke, and U. Peschel, Light-matter interaction and lasing in semiconductor nanowires: A combined finite-difference time-domain and semiconductor Bloch equation approach, Phys. Rev. B **91**, 045203 (2015).

[18] P. Földi, M. G. Benedict, and V. S. Yakovlev, The effect of dynamical Bloch oscillations on optical-field-induced current in a wide-gap dielectric, New J. Phys. **15**, 063019 (2013).

[19] P. Földi, Gauge invariance and interpretation of interband and intraband processes in high-order harmonic generation from bulk solids, Phys. Rev. B **96**, 035112 (2017).

[20] G. Ernotte, T. J. Hammond, and M. Taucer, A gauge-invariant formulation of interband and intraband currents in solids, Phys. Rev. B **98**, 235202 (2018).

[21] S. Datta, *Electronic Transport in Mesoscopic Systems* (Cambridge University Press, Cambridge, 1995).

[22] J. Nitta, T. Akazaki, H. Takayanagi, and T. Enoki, Gate Control of Spin-Orbit Interaction in an Inverted in GaAsInAlAs Heterostructure, Phys. Rev. Lett. **78**, 1335 (1997).

[23] M. P. Nowak, B. Szafran, and F. M. Peeters, Fano resonances and electron spin transport through a two-dimensional spin-orbit-coupled quantum ring, Phys. Rev. B **84**, 235319 (2011).

[24] C. Durkan, *Current at the Nanoscale: An Introduction to Nanoelectronics* (World Scientific, Singapore, 2014).

[25] K. Kolasiński, B. Szafran, B. Brun, and H. Sellier, Interference features in scanning gate conductance maps of quantum point contacts with disorder, Phys. Rev. B **94**, 075301 (2016).

[26] M. Patra and S. Maiti, Simultaneous spin-based boolean logic operations with reprogrammable functionality, Europhys. Lett **123**, 58008 (2018).

[27] Z.-G. Zhu and J. Berakdar, Photoinduced nonequilibrium spin and charge polarization in quantum rings, Phys. Rev. B **77**, 235438 (2008).

[28] V. K. Kozin, I. V. Iorsh, O. V. Kibis, and I. A. Shelykh, Quantum ring with the Rashba spin-orbit interaction in the regime of strong light-matter coupling, Phys. Rev. B **97**, 155434 (2018).

[29] J. B. Khurgin, Optically induced currents in dielectrics and semiconductors as a nonlinear optical effect, J. Opt. Soc. Am. B **33**, C1 (2016).

[30] K. E. Echternkamp, A. Feist, S. Schäfer, and C. Ropers, Ramsey-type phase control of free-electron beams, Nat. Phys. **12**, 1000 (2016).

[31] A. Feist, K. E. Echternkamp, J. Schauss, S. V. Yalunin, S. Schäfer, and C. Ropers, Quantum coherent optical phase modulation in an ultrafast transmission electron microscope, Nature (London) **521**, 200 (2015).

[32] M. Kozák, J. McNeur, K. J. Leedle, H. Deng, N. Schönenberger, A. Ruehl, I. Hartl, J. S. Harris, R. L. Byer, and P. Hommelhoff, Optical gating and streaking of free electrons with sub-optical cycle precision, Nat. Commun. **8**, 14342 (2017).

[33] L. Z. Szabó, M. G. Benedict, and P. Földi, Scattering of charged particles on two spatially separated time-periodic optical fields, Phys. Rev. A **96**, 063419 (2017).

[34] R. Landauer, Spatial variation of currents and fields due to localized scatterers in metallic conduction, IBM J. Res. Dev. **32**, 306 (1988).

[35] M. Büttiker, Symmetry of electrical conduction, IBM J. Res. Dev. **32**, 317 (1988).

[36] S. Jiang, H. Wei, J. Chen, C. Yu, R. Lu, and C. D. Lin, Effect of transition dipole phase on high-order-harmonic generation in solid materials, Phys. Rev. A **96**, 053850 (2017).

[37] M. Durach, A. Rusina, M. F. Kling, and M. I. Stockman, Metallization of Nanofilms in Strong Adiabatic Electric Fields, Phys. Rev. Lett. **105**, 086803 (2010).

[38] V. Hanus, V. Csajbók, Z. Pápa, J. Budai, Z. Márton, G. Z. Kiss, P. Sándor, P. Paul, A. Szeghalmi, Z. Wang, B. Bergues, M. F. Kling, G. Molnár, J. Volk, and P. Dombi, Light-field-driven current control in solids with pj-level laser pulses at 80 mHz repetition rate, Optica **8**, 570 (2021).

[39] V. Szaszkó-Bogár, P. Földi, I. Magashegyi, and K. Varjú, Interference-induced phenomena in high-order harmonic generation from bulk solids, Appl. Sciences (Basel) **9**, 1572 (2019).

[40] S. Ghimire, A. D. DiChiara, E. Sistrunk, P. Agostini, L. F. DiMauro, and D. A. Reis, Observation of high-order harmonic generation in a bulk crystal, Nat. Phys. **7**, 138 (2011).

[41] I. Magashegyi, L. Z. Szabó, and P. Földi, Ultrashort laser-pulse-driven currents in conductors: One-dimensional model for local excitation in the single-electron picture with quadratic dispersion, J. Opt. Soc. Am. B **35**, A116 (2018).